*Available online www.jocpr.com*

**Journal of Chemical and Pharmaceutical Research, 2016, 8(3):353-364**

**Research Article**

**ISSN : 0975-7384**
**CODEN(USA) : JCPRC5**

# Inhibition effect of 2-mercaptobenzothiazole on the corrosion of copper in 2M $HNO_3$

**D. Ehouman[1], J. S. Akpa[2], P. M. Niamien[1]*, D. Sissouma[2], A. Trokourey[1]**

*[1]Laboratoire de Chimie Physique, Université Félix Houphouët Boigny*
*[2]Laboratoire de Chimie Organique Structurale, Université Félix Houphouët Boigny, 22 BP582 Abidjan 22*

---

**ABSTRACT**

*2-Mercaptobenzothiazole (MBT) was examined as a corrosion inhibitor for copper corrosion in 2M nitric acid solution, using mass loss technique and quantum chemical studies, based on density functional theory(DFT) at B3LYP level with different basis sets including 6-31G (d), 6-31G (d, p), and LanL2DZ. The percentage inhibition efficiency IE (%) was found to increase with increasing inhibitor concentration and increasing temperature. Adsorption of the molecule on copper surface follows the modified Langmuir adsorption isotherm. The thermodynamic functions related to the adsorption and the activation processes were calculated and discussed. The calculated quantum chemical parameters correlated to the inhibition efficiency are the highest occupied molecular orbital energy ($E_{HOMO}$), the lowest unoccupied molecular orbital energy ($E_{LUMO}$), the HOMO-LUMO energy gap, hardness ($\eta$), softness (S), the dipole moment ($\mu$), the electron affinity (A), the ionization energy (I), the absolute electronegativity ($\chi$), the fraction ($\Delta N$) of electrons transferred from (MBT) to copper and the electrophilicity index ($\omega$). The local reactivity has been analysed through the condensed Fukui function and the condensed softness indices in order to determine the sites for nucleophilic and electrophilic attacks. Theoretical results and experimental ones are in well accordance.*

**Keywords**: Copper, nitric acid, 2-Mercaptobenzothiazole, corrosion inhibition, mass loss technique, DFT, Quantum chemical parameters.

---

## INTRODUCTION

Copper and its alloys [1- 3] are still widely used in many applications (marine, microelectronic industries, communication, pipelines, heat exchangers etc.)despite [4] the emergence in recent years of other materials that have technical and economical attractions. This is due to their excellent electrical and thermal conductivities associated to their good mechanical workability. Thus, corrosion of copper and its inhibition in a wide variety of media, particularly in acidic media [5-7] have attracted the attention of many investigators.

One of the most important methods in protection of copper against corrosion is the use of organic inhibitors [8-11] containing polar groups including nitrogen, sulphur and oxygen and heterocyclic compounds [12-15] with polar functional groups and conjugated double bonds. The inhibitory action of these organic compounds is attributed to their interactions with the copper surface via their adsorption. Polar functional groups [16] are regarded as the reaction centre that stabilizes the adsorption process. In general, the adsorption of an inhibitor on a metal surface [17] depends on the nature and the surface of the metal, the adsorption mode, the molecular structure and the type of the electrolyte solution.

Benzothiazole derivatives [18, 19] have been studied extensively for their diverse chemical reactivity and potential broad spectrum of biological activity. They are heterocyclic compounds widely found in bioorganic and medicinal chemistry with application in drug discovery.

Despite the widespread increasing interests in the application of these organic inhibitors, experimental results reveal different behaviour of the studied compounds in a given environment. The mean objective of theoretical research is to gain insight into the mechanisms by which inhibitor molecules added to aqueous environment retard the metal/corrodent interaction.

Density functional theory (DFT) [20] has been found to be successful in providing insights into the chemical reactivity and selectivity, in terms of global parameters such as electronegativity (χ) [21], hardness (η) [22] and softness (S) [20], and local ones such as the condensed Fukui function $f(r)$ [23] and the condensed local softness $s(r)$ [24].

In the present study, we will focus on the behaviour of 2-Mercaptobenzothiazole against copper corrosion in 2M nitric acid using mass loss technique and DFT.

## EXPERIMENTAL SECTION

### Copper specimens

The copper specimens were in form of rod measuring 10 mm in length and 2.2 mm of diameter; they were cut in commercial copper of purity 95%.

### The studied molecule

This organic compound with white colour has been synthesized in the laboratory. Its molecular structure has been identified by $^1$H NMR spectroscopy and mass spectroscopy.

NMR$^1$H (DMSOd-6, δ ppm): 3, 39 (1H, s, SH); 7, 25-7, 66 (3H, m, $H_{ar}$); 7, 66-7, 69 (1H, m, $H_{ar}$). SDM: m/e (%): 167 (15%); 168 (100%); 169 (10%).

Figure 1 gives the optimized chemical structure.

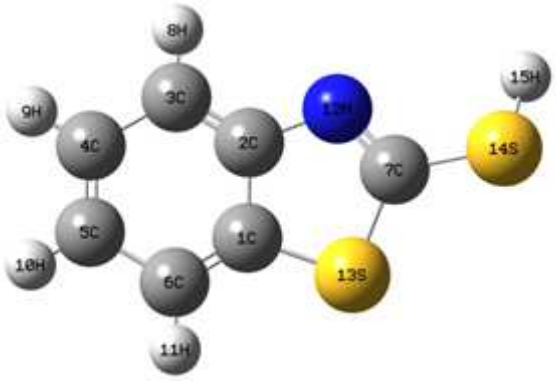


**Figure 1 Optimized chemical structure of MBT by B3LYP/6-31 G (d)**

### Solution

Analytical grade 65% nitric acid solution from Merck was used to prepare the corrosive aqueous solution. The solution was prepared by dilution of the commercial nitric acid solution using double distilled water. The blank was a 2 M $HNO_3$ solution.(MBT) solutions range from 0.01 to 0.5mM

### Mass loss method

The mass loss measurements were conducted under total immersion of the pre-weighed copper specimen in 100 mL capacity bakers containing 50 mL of the test solution. The specimen were retrieved 1 hour later and rinsed thoroughly with distilled water, cleaned, dried in acetone and reweighed using a balance with sensibility $\pm 0.1$ mg. The tests were run triplicate for different temperatures 308-328K and the standard deviation values among parallel triplicate experiments were found to be smaller than 3%, indicating reliability and reproducibility, and mean values of the mass loss data were used to compute parameters as corrosion rate, inhibition efficiency and degree of surface coverage using the following relations:

$$W = \frac{\Delta m}{St} \quad (1)$$

$$IE(\%) = \frac{W_0 - W}{W_0} \times 100 \quad (2)$$

$$\theta = \frac{W_0 - W}{W_0} \quad (3)$$

Where $W_0$ and $W$ are respectively the corrosion rate without and with (MBT), $\Delta m$ is the mass loss, $S$ is the total surface of the copper specimen and $t$ is the immersion time.

**Computational details**

Density functional theory (DFT) calculations were carried out using Becke three parameter nonlocal exchange functional [25] with the nonlocal correlation of Lee et al. [26] and Miehlich et al. [27] with three basis sets including 6-31 G(d), 6-31 G(d, p) and LanL2DZ implemented in the Gaussian 03 W program package [28]. Geometry optimization of the ground state with each of the three methods was carried out without imposing constraint. Relevant parameters were calculated in order to describe the molecular-metal interactions.

The basic relationship of density functional theory of chemical reactivity is precisely, the one established by Parr et al. [29] that links the electronic chemical potential $\mu_P$ with the first derivative of the energy with respect to the number of electrons, and therefore with the negative of the electronegativity $\chi$:

$$\mu_P = \left(\frac{\partial E}{\partial N}\right)_{v(r)} = -\chi \quad (4)$$

Hardness $(\eta)$ which measures both the stability and the reactivity of a molecule [30] has been defined as the second derivative of total energy $E$ with respect to $N$ at $v(r)$:

$$\eta = \left(\frac{\partial^2 E}{\partial N^2}\right)_{v(r)} = \left(\frac{\partial \mu_P}{\partial N}\right)_{v(r)} \quad (5)$$

In these equations, $\mu_P$ is the chemical potential, $E$ is total energy, $N$ is the number of electrons and $v(r)$ is the external potential.

According to Koopmans's theorem [31], the ionization energy *I* can be approximated as the negative of the highest occupied molecular orbital (HOMO) energy:

$$I = -E_{HOMO} \quad (6)$$

The negative of the lowest unoccupied molecular orbital (LUMO) energy is similarly related to electron affinity *A* as follows:

$$A = -E_{LUMO} \quad (7)$$

Electronegativity $(\chi)$ and hardness $(\eta)$ can then be written as:

$$\chi = \frac{I + A}{2} \quad (8)$$

$$\eta = \frac{I - A}{2} \quad (9)$$

The fraction of electrons transferred from the molecule to the metal [32] is expressed as follows:

$$\Delta N = \frac{\chi_{Cu} - \chi_{inh}}{2(\eta_{Cu} + \eta_{inh})} \quad (10)$$

The inverse of hardness is softness [24]:

$$S = \left(\frac{\partial N}{\partial \mu_P}\right)_{v(r)} \quad (11)$$

Global electrophilicity index$(\omega)$, introduced by Parr [33] which is a measure of energy lowering due to maximal electron flow between donor and acceptor is giving by:

$$\omega = \frac{\mu_p^2}{2\eta} \quad (12)$$

The local reactivity of the studied molecule can be analyzed through the condensed Fukui indices. The condensed Fukui functions indicate the atoms in a molecule that have a tendency to either donate (nucleophile character) or

accept (electrophile character) an electron or pair of electrons. The nucleophilic and electrophilic functions can be computed using the finite difference approximation as follows:

$$f_k^+ = q_k(N+1) - q_k(N) \quad (13)$$

$$f_k^- = q_k(N) - q_k(N-1) \quad (14)$$

In equations (13) and (14), $q_k$ is the gross charge of atom $k$ in the molecule and $N$ is the number of electrons.

## RESULTS AND DISCUSSION

### Mass loss experiment

Mass loss data were determined at the end of 1 hour time interval in the absence and presence of different concentrations of (MBT) and were used to calculate corrosion rates, inhibition efficiency and degree of surface coverage as provided by equations (1) to (3). Figures 1 and 2 show respectively the evolution of corrosion rate and inhibition efficiency with respect to temperature and (MBT) concentration.

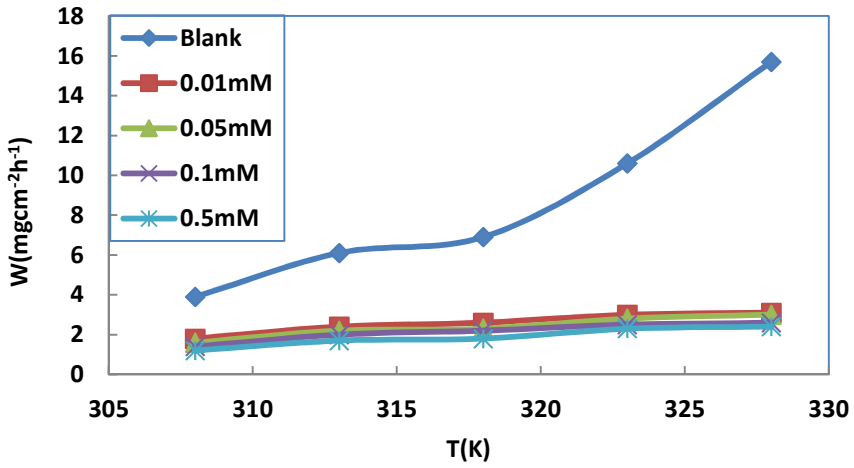


**Figure 1 Corrosion rate versus temperature for different concentrations of (MBT)**

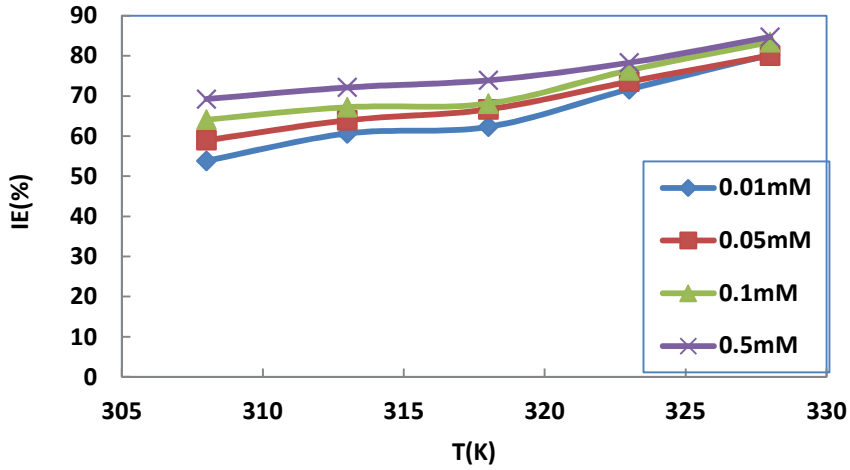


**Figure 2 Inhibition efficiency versus temperature for different concentrations of (MBT)**

Figure 1 shows that corrosion rate increases with increasing temperature but decreases with increasing concentration of (MBT). A plausible explanation of these results is that the increasing inhibitor's concentration reduces the copper exposed surface to the corrosive media through the increasing number of adsorbed molecules on its surface which hinder the direct attack on the metal surface. Analyzing figure 2 one can see that inhibition efficiency increases with increasing temperature and concentration. Similar observation [34] has been seen in the literature and supports the idea that the adsorption of the inhibitor onto the copper surface is chemical in nature.

**Adsorption considerations**

In order to ascertain and quantitatively describe certain parameters associated with the adsorption behavior of (MBT) on copper surface, the degree of surface coverage $\theta$ of the molecule was fitted into adsorption isotherms and the model that best fits to the adsorption process was chosen using correlation coefficient $R^2$ values of the plots: the highest value of correlation coefficient corresponds to the best model. The isotherms models in their respective ways are described by the following equation:

$$f(\theta,x)\exp(-2a\theta) = K_{ads}C_{inh} \quad (15)$$

Where $f(\theta,x)$ represents the configuration factor and depends on the physical model and the assumptions underlying the derivation of the model, $\theta$ is the degree of surfacecoverage,$C_{inh}$ is the concentration of the inhibitor in the aggressive medium, $x$ is the size ratio, $a$ is the molecular interaction parameter and $K_{ads}$ is the equilibrium constant of the adsorption process. The equations of the attempted models are listed in table 1.

**Table1 Equations of the studied isotherms**

| Isotherm | Equation |
|---|---|
| Langmuir | $\frac{C_{inh}}{\theta} = \frac{1}{K_{ads}} + C_{inh}$ |
| Flory-Huggins | $log\left(\frac{\theta}{C_{inh}}\right) = logxK + xlog(1-\theta)$ |
| El-Awady | $log\left(\frac{\theta}{1-\theta}\right) = logK + ylogC_{inh}\left(K_{ads} = K^{1/y}\right)$ |

**Figures 3 (A, B and C) give the plots of the studied isotherms**

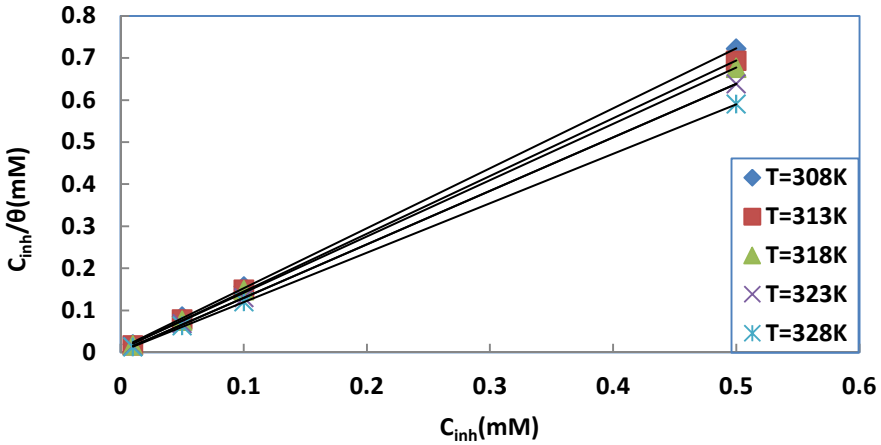


**Figure 3 A Langmuir adsorption plots of (MBT) on copper in 2M $HNO_3$ for different temperatures**

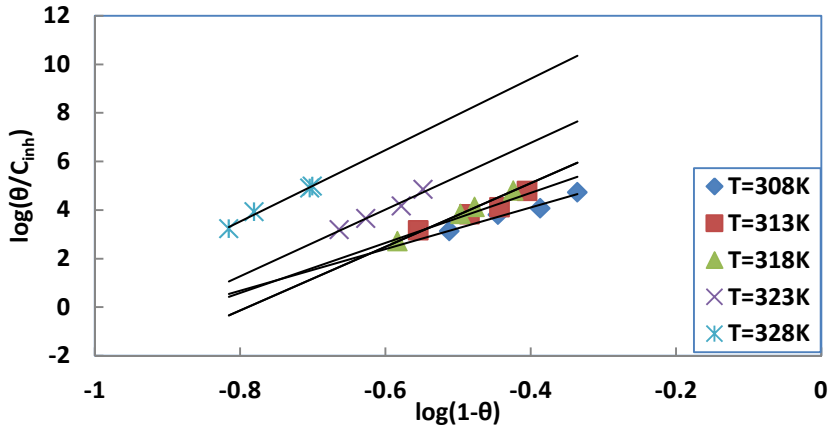


**Figure 3 B Flory Huggins adsorption plots of (MBT) on copper in 2M $HNO_3$ for different temperatures**

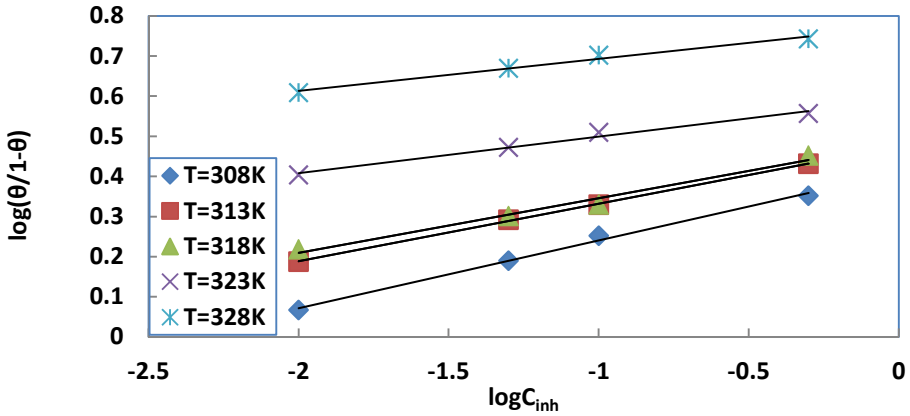


**Figure 3 C El-Awady adsorption plots of (MBT) on copper in 2M $HNO_3$ for different temperatures**

Langmuir adsorption isotherm is by far the best isotherm ($R^2$ is nearly equals to unity) but there is divergence of the slope from unity [35] due to interactions between adsorbed species on the copper surface as well as changes in the values of the Gibbs energy with increasing surface coverage. The results suggest a slight deviation from ideal conditions (all the adsorption sites are equivalent) assumed in the Langmuir model. Therefore, a modified Langmuir equation suggested elsewhere [36] given in the equation below that takes care of this deviation may be used:

$$\frac{C_{inh}}{\theta} = \frac{n}{K_{ads}} + nC_{inh} \qquad (16)$$

Thermodynamic parameters can be determined using the relationship between the equilibrium constant $K_{ads}$ and the adsorption free enthalpy change $\Delta G^0_{ads}$:

$$\Delta G^0_{ads} = -RTln(55.5K_{ads}) \qquad (17)$$

Where $R$ is the perfect gas constant, T is the absolute temperature and 55.5 is the concentration of water in mol $L^{-1}$. The obtained values of $\Delta G^0_{ads}$ are summarized in table 2.

**Table 2 Adsorption thermodynamic functions**

| T(K) | $K_{ads}(\times 10^2 M^{-1})$ | $\Delta G^0_{ads}(kJ\ mol^{-1})$ | $\Delta H^0_{ads}(kJ\ mol^{-1})$ | $\Delta S^0_{ads}(J\ mol^{-1}K^{-1})$ |
|---|---|---|---|---|
| 308 | 7.015 | -27.06 | 7.78 | 113 |
| 313 | 7.287 | -27.59 | | |
| 318 | 7.468 | -28.10 | | |
| 323 | 7.868 | -28.68 | | |
| 328 | 8.502 | -29.34 | | |

The negative values of $\Delta G^0_{ads}$ indicate the spontaneity of the adsorption process and the stability of the adsorbed layer on the copper surface. Generally [37] values of $\Delta G^0_{ads}$ up to -20 kJ $mol^{-1}$ are consistent with physisorption, while those around - 40 kJ $mol^{-1}$ or more negative are associated with chemisorption as a result of the sharing or transfer of electrons from the organic molecule to the metal surface to form a coordinate bond. The calculated values of $\Delta G^0_{ads}$ show that the adsorption mechanism of (MBT) on copper involves both physisorption and chemisorption.The standard enthalpy ($\Delta H^0_{ads}$) and entropy ($\Delta S^0_{ads}$) changes are deduced using the equation below:

$$\Delta G^0_{ads} = \Delta H^0_{ads} - T\Delta S^0_{ads} \qquad (18)$$

Where $\Delta H^0_{ads}$ and $(-\Delta S^0_{ads})$ are respectively the intercept and the slope of the straight line obtained when plotting $\Delta G^0_{ads}$ versus temperature (figure 4).

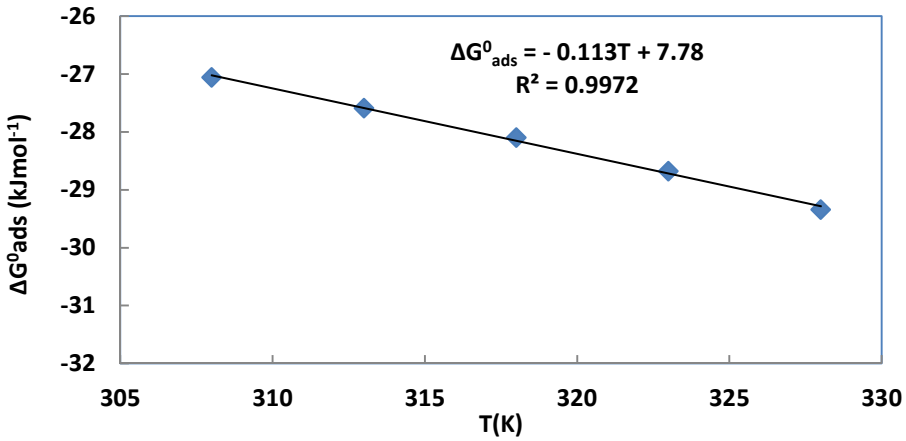


**Figure 4 Free enthalpy changes versus temperature**

The positive value of $\Delta H^0_{ads}$ indicate that the adsorption of the inhibitor is an endothermic process. Literature [38] pointed out that an exothermic process signifies either physisorption or chemisorption while an endothermic process is associated to chemisorption. The values of $\Delta S^0_{ads}$ are positive indicating an increase in disorder what can be explained by a desorption of water molecules.

**Effect of temperature**

In order to calculate activation parameters for the corrosion process, Arrhenius equation and transition state equation [39] were used:

$$logW = logA - \frac{E_a}{2.303RT} \quad (19)$$

$$log\left(\frac{W}{T}\right) = \left[log\left(\frac{R}{\aleph h}\right) + \frac{\Delta S^*_a}{2.303R}\right] - \frac{\Delta H^*_a}{2.303RT} \quad (20)$$

Where $W$ is the corrosion rate, $R$ is the perfect gas constant, $T$is the absolute temperature, $A$ is the pre-exponential factor, $h$ is the Plank's constant and $\aleph$ is the Avogadro's number.

Figure 5 depicts the Arrhenius plots, log against 1/T for copper in 2M $HNO_3$ without and with different concentrations of (MBT). Straight lines are obtained with very high correlation coefficients ($R^2 > 0.9$). The slopes $\left(-\frac{E_a}{2.303R}\right)$ of these straight lines allow the calculations of the apparent activation energy($E_a$). The obtained values are collected in table 3.

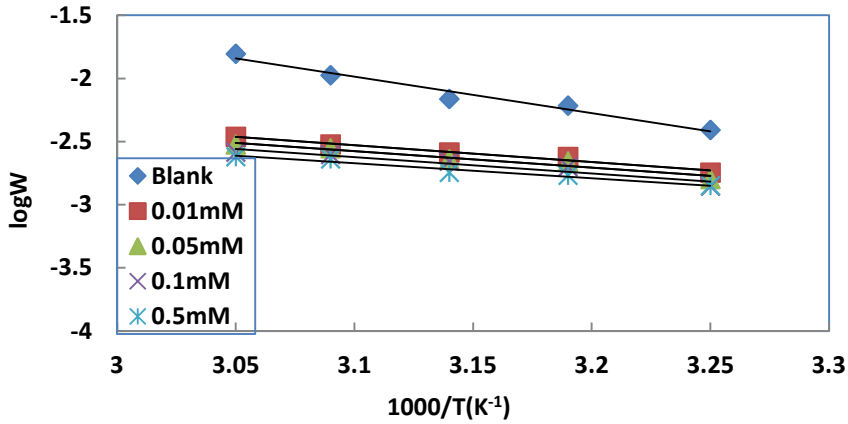


**Figure 5 $logW$ versus $1/T$ for the corrosion of copper in 2M $HNO_3$with and without (MBT)**

**Table 3 Activation parameters for copper dissolution in 2M $HNO_3$ in the absence and presence of different concentrations of (MBT)**

| Solution | $E_a(kJ\ mol^{-1})$ | $\Delta H_a^*(kJ\ mol^{-1})$ | $\Delta S_a^*(J\ mol^{-1}K^{-1})$ |
|---|---|---|---|
| Blank | 55.01 | 52.47 | -120.8 |
| 0.01mM | 25.55 | 23.03 | -222.5 |
| 0.05mM | 25.16 | 22.52 | -224.9 |
| 0.1mM | 24.80 | 22.13 | -227.1 |
| 0.5mM | 22.67 | 19.95 | -234.8 |

The calculated $E_a$ for the blank is higher than that of solutions containing (MBT). The increase in IE (%) with increasing temperature and the lower values of activation energies in presence of (MBT) [40] can be interpreted as an indication for chemical adsorption.Figure 6 shows the plots of $log\ (W/T)$ against (1/T).

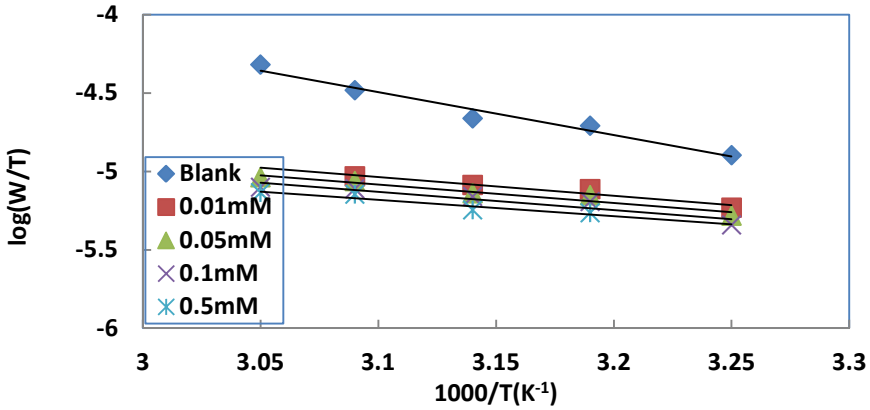


**Figure 6 $log(W/T)$ versus $(1/T)$ for copper corrosion in 2M $HNO_3$ with and without (MBT)**

The obtained values of $\Delta H_a^*$ and $\Delta S_a^*$ are listed in table 3. The positive values of $\Delta H_a^*$reflects the endothermic process of dissolution of copper. The negative value of $\Delta S_a^*$ [41] shows that there is a decrease in disorder as the reactants are converted into the activated complexes.

**Quantum chemical calculations using DFT method**

We have computed chemical descriptors of the molecule using DFT at B3LYP level with basis sets including 6-31 G (d), 6-31 G (d, p) and LanL2DZ. The choice of the best method was based on CPU times and total energy according to the variational principles which states that the ground state energy is the minimum energy:

$$E = min_n[F(n) + \int d^3r\, V_{ext}(r)n(r)] \qquad (21)$$

Where $F(n)$, $V_{ext}(r)$ and $n(r)$ are respectively a universal functional, the external potential and the electronic density. Table 4 contains CPU time and the total energy of the molecule in respect of each method.

**Table 4 CPU time and total energy of the molecule with respect to the basis set**

| | 6-31 G(d) | 6-31 G(d, p) | LanL2DZ |
|---|---|---|---|
| CPU time | 1h14'56'' | 1h32'15'' | 37'30'' |
| Total energy (au) | -1120.89 | -1120.90 | -344.63 |

One can see from table 4 that the best method is B3LYP/6-31 G (d) which has the lowest CPU time and a total energy nearly equals to that of B3LYP/6-31G (d, p). Thus, all the descriptors of the molecule were computed using the chosen basis set.

The energy of highest occupied molecular orbital ($E_{HOMO}$) [42] measures the tendency towards the donation of electron by a molecule. Therefore, higher values of $E_{HOMO}$ indicate better tendency towards the donation of electron, enhancing the adsorption of the inhibitor on copper and therefore better inhibition efficiency. The lowest unoccupied molecular orbital energy ($E_{LUMO}$) indicates the ability of the molecule to accept electrons. So, the binding ability of the inhibitor to the metal surface increases with increasing $E_{HOMO}$ and decreasing $E_{LUMO}$. The optimized molecular structure of (MBT) with Mulliken charges on atoms is given by figure 7.

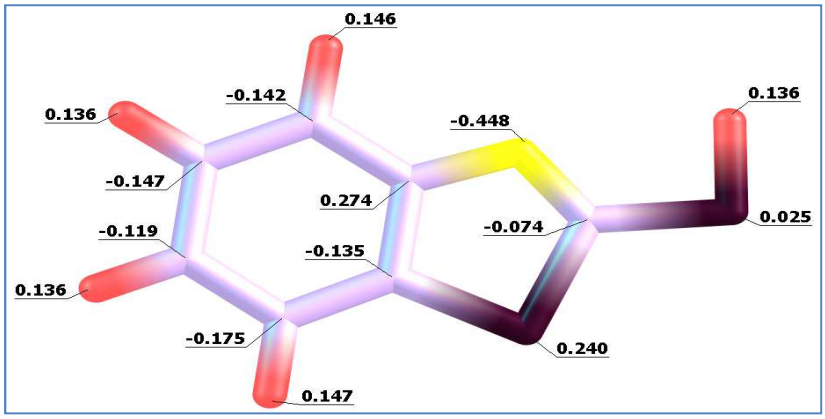


**Figure 7 Mulliken charges on atoms of (MBT) by B3LYP/6-31 G (d)**

Figure 8 shows the highest occupied molecular orbital (HOMO) and the lowest unoccupied molecular orbital (LUMO) of the molecule under study.

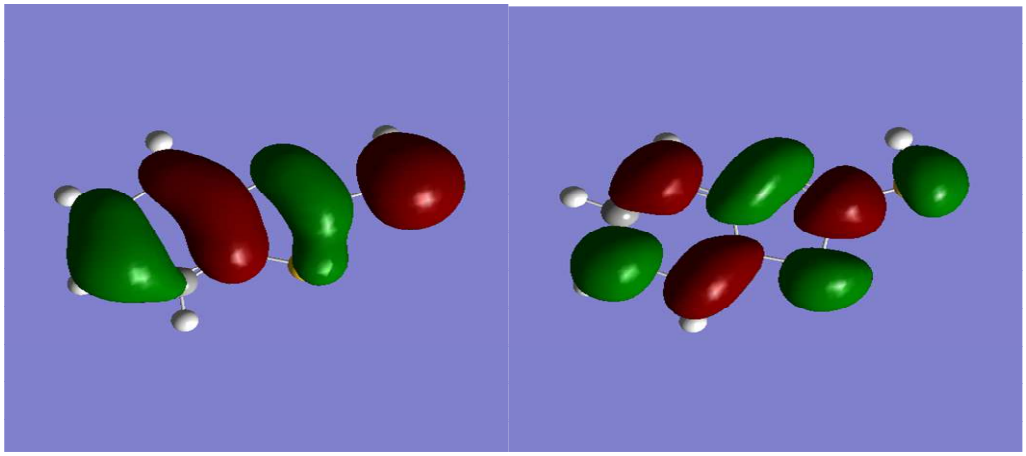

**Figure 8 HOMO (left) and LUMO (right) of (MBT) by DFT/ B3LYP/6-31G(d)**

The analysis of Figure 8 shows that the density of HOMO and LUMO are distributed throughout (MBT) rings. The calculated quantum chemical parameters are collected in table 5.

**Table 5 Quantum chemical descriptors of (MBT)**

| Descriptor | Value | Descriptor | Value |
|---|---|---|---|
| $E_{HOMO}\ (eV)$ | -6.204 | $\chi(eV)$ | 3.594 |
| $E_{LUMO}\ (eV)$ | -0.984 | $\eta(eV)$ | 2.610 |
| $\Delta E\ (eV)$ | -5.220 | $S(eV)^{-1}$ | 0.383 |
| $\mu\ (D)$ | 1.0071 | $\Delta N$ | 0.265 |
| $I(eV)$ | 6.204 | $\omega$ | 2.474 |
| $A(eV)$ | 0.984 | $E_N(au)$ | -1120.89 |

The energy gap ($\Delta E = E_{LUMO} - E_{HOMO}$) is an important parameter as a function of reactivity of the inhibitor molecule towards the adsorption on the metal surface. As $\Delta E$ decreases the reactivity of the molecule increases leading to increase in inhibition efficiency of the molecule. Lower values of the energy gap [43] will render good inhibition efficiency, because the energy to remove an electron from the last orbital will be low. The dipole moment μ is another important electronic parameter resulting from non-uniform distribution of charge on atoms in the molecule.

In literature, some authors state that lower values of dipole moment [44] will favour accumulation of the inhibitor in the surface layer and therefore inhibition efficiency. However, many researchers [45, 46] state that the inhibition efficiency increases with increasing values of dipole moment. In general [47] there is no significant relationship between the dipole moment and the inhibition efficiency.

Ionization energy is also an important descriptor of chemical reactivity of atoms and molecules. High ionization energy [47] leads to high stability and chemical inertness and small ionization energy is associated to high reactivity of atoms and molecules. In the work herein, the low ionization energy (6.204 eV) of (MBT) probably explains its good inhibition efficiency.

Absolute hardness and softness are important properties to measure the molecular stability and reactivity. The chemical hardness represents the resistance towards the deformation or polarization of the electron cloud of the atoms, ions or molecules under small perturbation or chemical reaction. A hard molecule [48] has a large energy gap and a soft molecule has small energy gap. In our work, the low hardness value of (MBT) (2.610 eV) compared with many other compounds, reflects its good performance as a corrosion inhibitor of copper in the studied medium. It is evident that in that case the softness value (0.383 $eV^{-1}$) is high since softness is the inverse of hardness.

To calculate the fraction of electrons transferred, the theoretical values $\chi_{Cu} = 4.98\ eV$ [49] and $\eta_{Cu} = 0$ [50] were used. The value of the number of electrons transferred ($\Delta N = 0.265$)obtained can be used [51] toshow that the inhibition efficiency result from electron donation.

The electrophilicity index (ω) expresses the ability of the inhibitor to accept electrons. In our work (ω = 2.474); this larger value indicates a good capacity of (MBT) to accept electrons from copper.

The Mulliken charge densities calculated from the optimised geometry of (MBT) reveal that most of the carbon atoms**C1** (-0.135e), **C3** (-0.142e), **C4** (-0.147e), **C5** (-0.119e), **C6** (-0.175e),**C7** (-0.074e) and the nitrogen atom **N12** (-0.448e) which carry negative charges [52] may be used for forming bond with positively charged metal atoms on the surface.

The values of Fukui function and local softness for nucleophilic and electrophilic attacks are collected in table 6.

**Table 6 Condensed Fukui functions and local softness values for (MBT)**

| Number | Atom | $f_k^+(r)$ | $f_k^-(r)$ | $S_k^+(r)$ | $S_k^-(r)$ |
|---|---|---|---|---|---|
| 1 | C | 0.008214 | -0.021147 | 0.00314596 | -0.00809930 |
| 2 | C | **0.009410** | -0.032018 | **0.00360403** | -0.01226281 |
| 3 | C | -0.034374 | -0.051852 | -0.01316524 | -0.01985932 |
| 4 | C | 0.001376 | -0.016774 | 0.00052701 | -0.00642444 |
| 5 | C | -0.032372 | -0.041226 | -0.01239848 | -0.01578956 |
| 6 | C | -0.019732 | -0.021823 | -0.00755736 | -0.00835821 |
| 7 | C | -0.067745 | **0.004072** | -0.02594634 | **0.00155958** |
| 8 | H | -0.067537 | -0.073362 | -0.02586667 | -0.02809765 |
| 9 | H | -0.070645 | -0.077648 | -0.02705704 | -0.02973918 |
| 10 | H | -0.075064 | -0.084773 | -0.02874951 | -0.03246806 |
| 11 | H | -0.063934 | -0.071149 | -0.02448672 | -0.02725007 |
| 12 | N | -0.058645 | -0.042903 | -0.02246104 | -0.01643185 |
| 13 | S | -0.204309 | -0.171828 | -0.07825035 | -0.06581012 |
| 14 | S | -0.180800 | -0.247189 | -0.06924640 | -0.09467339 |
| 15 | H | -0.143840 | -0.050382 | -0.05509072 | -0.01929631 |

In DFT, the so called Fukui functions are advocated as reactivity descriptors in order to identify the most reactive sites for electrophilic or nucleophilic reactions within a molecule. The most common expression is [20]:

$$f(r) = \left(\frac{\partial \rho(r)}{\partial N}\right)_{V_{ext}} \quad (22)$$

They reflect the change in electron density at a point $r$ with respect to a change in number of electrons $N$, under constant external potential $V_{ext}$. Molecular properties are often associated with a certain point in space. It is then necessary to identify an atom in the molecule. The difficulty is that there is not yet an operator [53] which, acting on the wave function or electron density, can perform a division of the space in atomic basins. Despite this fundamental problem, Fukui functions are often condensed to atomic resolution. These condensed Fukui functions (equations (13) and (14)) are in the context of variational approach to chemical reactivity, more instructive indicators of molecular site reactivity than Fukui function (equation (22)). According to the values of the computing functions, one can see from table 6 that nucleophilic attacks take place around the carbon atom **C2**whereas the electrophilic attacks are located around the carbon atom **C7**.

**Acknowledgements**
The authors are grateful to the Central Laboratory of Agrochemical and Ecotoxicology of Abidjan (Côte d'Ivoire) for providing the facilities to carry out the work.

## CONCLUSION

The following conclusions can be drawn from the study:
1. (MBT) acts as a good corrosion inhibitor of copper in 2M $HNO_3$.
2. Inhibition efficiency is concentration and temperature dependent.
3. (MBT) adsorbs on copper according to the modified Langmuir isotherm.
4. The calculated thermodynamic parameters related to the adsorption and the activation indicated a chemical type of adsorption.
5. Quantum chemical parameters confirm the inhibition efficiency of (MBT).
6. Fukui condensed functions show the nucleophilic and the electrophilic sites in the molecule.

## REFERENCES

[1] G KJennings and P E Laibinis,*Colloids and Surfaces A: Physicochem& Eng. Asp*., **1996**,116,105-114.
[2] HY Ma; C Yang; B S Yin ; G Y Li; S H Chen and J L Luo, *Appl.Surf.Sci.,* **2003**, 218,144-154.
[3] EISayed and M Sherif, *Appl. Surf.Sci*., **2006**, 252, 8615-8623.
[4] PT Gilbert, *Materials Performance*, **1982**, 21, 47-53.
[5]I Numez; E Reguera; F Corvo; E Gonzalez and C Vasquez, *Corros. Sci*., **2005**, 47, 461- 484.
[6] E Rocca; G Bertrand; C Rapin and J C Labrune, *J. Eletroanal. Chem*., **2001**, 503, 133-140.
[7] AG Christy; A Lowe; V Otieno-Alego; M Stoll and R D Webster, *J. Appl. Electrochem*., **2004** 34, 225- 233.
[8] DG Zhang; I X Gao and G D Zhou, *J. Appl. Surf.* Sci., **2004**, 225, 287-293.
[9] H Otmacic; J Telegdi; K Papp and E Stupnisek-Lisac, *J. Appl. Electrochem*., **2004**, 34, 545-550.
[10] F Zucchi; G Trabanelli and M Fonsati, *Corros. Sci*., **1996**, 38, 2019-2029.
[11] C Wang; S Chen and S Zhao, J. Electrochem. Soc., **2004**, 151, B11-B15.
[12] H Otmacic and E Stupnisek-Lisac, *Electrochim. Acta*, **2002**, 48, 985-991.
[13] M A Elmorsi and A M Hassanein, *Corros. Sci*., **1999**, 41, 2337-2352.
[14] M Scendo; D Poddebnick and J Malyszko, *J. Appl. Electrochem*., **2003**, 33, 287-293.
[15] A Dafali; B Hammouti; R Touzani; S Kertit; A Ramdani and K El Kacemi, *Anti-Corros.Method Mater*, **2002**, 49, 96-104.
[16] MG Fontana and K W Staehle, *Advances in corrosion Science and Technology*, vol 1, Plenum Press, New York, **1970**.
[17] O I Riggs, Jr., *Corrosion inhibitors*, 2nd ed., C C Nathan, Houston, TX, **1973**.
[18] H L K Stanton; R Gambari; H C Chung; C O T Johny; C Filly and S C C Albert, *Bioorg Med.*,*Chem*.,**2008**, 16,3626-3631.
[19] M Wang; M Gao; B Mock; K Miller; G Sledge; G Hutchins and Q. Zheng, *Bioorg MedChem*., **2006**, 14, 8599-8607.
[20] R G Parr and W Yang, *Density Functional Theory of Atoms and Molecules*, Oxford University Press: Oxford, U.K., **1989**.
[21] K D Sen, *Electronegativity, Structure and Bonding 66*, Springer Verlag, Berlin, **1987**.
[22] K D Sen, *Chemical Hardness, Structure and Bonding 80*, Springer Verlag: Berlin, **1993**.
[23] R G Parr and W Yang, *J. Am. Chem. Soc*. **1984**, 106, 4049-4050.
[24] WYang and R G Parr, *Proc. Natl. Acad. Sci.* U.S.A., **1985**, 82, 6723 - 6726.
[25] AD Becke, *J. Chem. Phys*., **1993**, 98, 5648-5652.
[26] C Lee; W Yang and R G Parr, *Phys. Rev. B*., **1988**, 37, 785-789.
[27] B Miehlich, A Savin, H Still, H Preuss, *Chem. Phys. Lett*., **1989**, 157, 200-206.
[28] M J Jr Frisch;G W Trucks;H B Schlegel; G E Scuseria; M A Robb; J R Cheeseman; J A Montgomery; T Vreven; K N Kudin; J C Burant; J M Millam; S S Iyengar ; J Tomasi;V Barone;B Mennucci;M Cossi;G Scalmani;N Rega;G A Petersson;H Nakatsuji;M Hada;M Ehara;K Toyota;R Fukuda;J Hasegawa;M Ishida;T Nakajima;Y Honda;O Kitao;H Nakai;M Klene;X Li, J E Knox;H P Hratchian;J B Cross;C Adamo;J Jaramillo;R Gomperts;R E Stratmann;O Yazyev;A J Austin;R Cammi;C Pomelli;J W Ochterski;P Y Ayala;K Morokuma;G A Voth;P Salvador;J J Dannenberg;V G Zakrzewski;S Dapprich;A D Daniels;M C Strain;O Farkas;D K Malick;A D Rabuck;K Raghavachari;J B Foresman;J V Ortiz;Q Cui;A G Baboul;S Clifford;J Cioslowski;B B Stefanov;G Liu;A Liashenko;P Piskorz;I R L Komaromi Martin;J Fox D ;T Keith ; M A Al-Laham;C Y Peng;A Nanayakkara;M Challacombe;P M W Gill;B Johnson;W Chen;M W Wong;C Gonzalez;J A Pople,*Gaussian 03,Revision B.05, Gaussian, Inc., PittsburghPA*, **2003**.
[29] R G Parr; R A Donnelly; M Levy; W E Palke, *J. Chem. Phys*., **1978**, 68, 3801-3807.

[30] R G Parr; R G Pearson, *J. Am. Chem. Soc*., **1983**, 105, 7512-7516.
[31]T Koopmans, *Physica (Elsevier),***1934**, 1, 104-113.
[32] R G Pearson, *Inorg. Chem*.,**1988**, 27, 734-740.
[33] R G Parr; L Szentpaly and S Liu, *J. Am. Chem. Soc*.,**1999**, 121, 1922-1924.
[34] I B Obot; N O Obi-Egbedi and S A Umoren, *Corrosion Science*,**2009**, 51, 1868-1875.
[35] E A Essien; S A Umoren; E E Essien and A P Udoh, *J. Mater. Environ. Sci*., **2012**, 3, 477 – 484.
[36] R F Villamil; P Corio; J C Rubin and SML Agostinho, *J. Electroanal. Chem*., **1999**, 472, 112-119.
[37] G Moretti; F Guidi and G Grion, *Corros. Sci*., **2004**, 46, 387- 403.
[38] W Durnie; R De Marco; A Jefferson and B Kinsella, J. Electrochem. Soc., **1999**, 146, 1751-1756.
[39] J O M Bockris and A K N Reddy, Modern Press, New York, **1977**, p. 1267.
[40] I Dehri and M Ozcan, *Mater. Chem. Phys.*, **2010**, 123, 666-677.
[41] H Zarrok; A Zarrouk; B Hammouti; R Salghi; C Jama and F Bentiss, *Corros. Sci*., **2012**, 64, 243-252.
[42] HE El Ashry; A El Nemr; S A Esawy and S Ragab, *Electrochimica Acta*, **2006,** 51, 3957-3968.
[43] IB Obot; N O Obi-Egbedi and S A Umoren, *Int. J. Electrochem. Sci*., **2009**, 4, 863-877.
[44] N Khalil, *Electrochimica Acta*, **2003**, 48, 2635-2640.
[45] K F Khaled; K Babic-Samardzija, N Hackerman, *Electrochimica Acta*, **2005**, 50, 2515-2520.
[46] G Bereket; E Hür and C Oretir, *Journal of Molecular Structure THEOCHEM*, **2002**, 578, 1-3.
[47] G Gece, *Corros. Sci*., **2008**, 50, 2981-2992.
[48] N O Obi-Egbedi; I B Obot; M I El-Khaiary; S A Umoren and E E Ebenso, *Int. J. Electrochem. Sci*., **2011**, 6, 5649-5675.
[49] R G Pearson, *Proc. Natl. Acad. Sci. USA*,**1986**, 83, 8440-8441.
[50] V S Sastri and J R Perumareddi, *Corrosion*, **1997**,53,617- 622.
[51] I Lukovits; E Kalman and F Zucchi, Corrosion **2001**, 57, 3-8.
[52] Y Karzani; El-Alaoui Belghiti; A Dafali and B Hammouti, *Journal of Chemical andPharmaceutical Research*, **2014**, 6, 689-696.
[53] P Bultinck; R Carbo-Dorca and W Langenaeker, *Journal of Chemical Physics*, **2003**, 118, 4349-4356.